Landslide susceptibility by mathematical model in Sarno area.

G. Capparelli[1], P. Versace[1],

[1] Department of Environmental and Chemical Engineering, University of Calabria - Arcavacata di Rende (CS) - Italy

Correspondence to: G. Capparelli (giovanna.capparelli@unical.it)

Abstract

Rainfall is recognized as a major precursor for many types of slope movements. Technical literature reports many examples both of study cases and models related to landslides induced by rainfall. Subsurface hydrology has a dominant role since changes in the soil water content affect significantly the soil shear strength. The analytical approaches are very different, ranging from statistical models to distributed models and complete, these last ones able to take several components into account, including specific site conditions, mechanical, hydraulic and physical soil properties, local seepage conditions, and the contribution of these to soil strength. The paper reports a study carried out by using a complete model, named SUSHI (Saturated Unsaturated Simulation for Hillslope Instability), on a case of great interest both for the complexity of the phenomenon and the severity with which it occurred.

The landslide-prone area is located in Campania region (Southern Italy), were disastrous mud-flows occurred in May 1998. The region has long been affected by rainfall-induced slope instabilities that often involved large areas, causing many victims. The applications allowed understanding better the role of the rainfall infiltration and of the suction changes in the triggering mechanism of the phenomena. These changes must be carefully considered when dealing with slope stability conditions for assessing hazard conditions and planning engineering works.

1 Introduction

The problems and the damages caused by landslides become complex and worrisome, accounting each year for huge property damage in terms of both direct and indirect costs. Social and economic losses due to landslides can be reduced by means of effective planning and management. The approaches include actions like the limitation of development in landslide-prone areas, the use of appropriate construction rules, the use of physical measures to prevent or control landslides and the setting up early warning systems. To address solutions to the landslide problem, it is necessary to develop a better understanding of landslide hazard regard the trigger mechanisms, propagation and impact structures.

Landslides can be attributed to a number of factors, such as geologic features, topography, vegetation, weather, or their combinations. Among the factors which contribute to the occurrence of these phenomena, rainfall is one of the most important.

As a result of rainfall events and subsequent infiltration into the subsoil, the soil moisture can be significantly changed with a decrease in matric suction in unsaturated soil layers and/or increase in pore-water pressure in saturated layers. As a consequence, in these cases, the shear strength can be reduced enough to trigger the failure.

The occurrence of the phenomena is also influenced by heterogeneity of hydraulic and geotechnical properties and water interaction. The complex hydrological responses of natural slopes are strongly influenced by the infiltration into unsaturated soil, generation of surface runoff, slope-parallel flow of a perched groundwater table, subsurface flow from upstream area, effect of vegetation, flow through macropores and discontinuities and into fractured bedrock. All these issues affect the predictive ability of the simulation models and, sometimes, the comprehension of the phenomena they can provide.

In addition, the shear strength contribution from soil suction above the groundwater table is usually ignored if the major portion of the slip surface is below the groundwater table. But negative pore water pressures can no longer be ignored in situations characterized by deep ground water table and shallow failure surface (Lu and Godt, 2013).

Technical literature reports many analytical approaches that differ for: the spatial scale range adopted that varies from wide area, up to ten of thousands kilometers, to small area, that can be reduced to a single landslide; the quality and quantity of hydrologic, hydraulic and geotechnical available data; the adopted detail for describing the hydrological and geotechnical mechanisms in slope.

Very popular models are the hydrological models that directly analyze the rainfall identifying the threshold values. These values are assumed on the basis of historical available data, are drawn in the intensity-duration plot as proposed by Caine (1980) and provide lower limit of rainfall associated to the occurrence of landslides, shallow landslides and debris flows (Guzzetti, 2008).

Other types of rainfall thresholds (Glade, 2000; Rahardjo et al., 2001) consider the effect of the antecedent rainfall precipitation more important than the rainfall recorded on the day of landslide occurrence. Usually this type of approach is related to the study of more complex landslides. The influence of antecedent rainfall on the slope stability is a topic of discussion (Martelloni et al., 2011).

These models are an important tool to support the prediction of landslides, applicable for early warning system (Capparelli & Tiranti 2010) and over wide areas. However, they don't provide any information about the hydrological processes involved in a landslide area and don't improve our understanding of landslide dynamics.

On the contrary, complete models can help in understanding triggering mechanisms since they attempt to reproduce the physical behavior of the processes involved at hillslope scale, employing detailed hydrological, hydraulic and geotechnical information (Montgomery and Dietrich, 1994; Pack et al., 1998; Rigon et al, 2006;Tsai et al., 2008).

These models develop analysis over wide areas and usually produce a susceptibility map characterizing the landslide prone zones according to a stability index. They are generally composed by an hydrological and geotechnical module. While the computation of the safety factor, in most cases, is performed by the limit equilibrium method, under the assumption of infinite slope, the hydrological modules present substantial differences.

The approach proposed in Shalstab (Montgomery and Dietrich, 1994) supposes a constant infiltration rate, neglects soil moisture above the water table, does not take into account the transient response to rainfall and considers the groundwater flows parallel to the slope. The assumptions are too restrictive, for example, when pore water pressure responds very quickly to transient rainfall and its redistribution has a large component normal to slope.

Wu and Sidle (1995) combined also the infinite slope equation with a subsurface flow model based on the kinematic wave approximation, taking also into account the vegetation root strength. An enhanced version of this model is proposed by Dhakal and Sidle (2004) that investigate the influence of different rainfall characteristics on slope stability.

Iverson (2000) developed a flexible modeling framework by modeling a one-dimensional linear diffusion process in saturated soil and using an analytical solution of the Richards equation. The model is valid for hydrological modeling in nearly saturated soil. According to this hypothesis, established to find an analytical solution of pressure heads, the infiltration capacity is assumed to be equivalent to the saturated hydraulic conductivity, instead of considering it as variable with time during the rainfall event. Furthermore, the Author considers ground surface of hillslope subject to a uniform rainfall.

For taking into account the variability of rainfall intensity and duration, dynamic or quasi-dynamic models have been introduced (Baum et al. 2002). The model, TRIGRS 1.0, allows a more precise description of slope hydrology but requires a large number of parameters.

Recently, TRIGRS 2.0 (Baum et al., 2010) allows calculating the filtration process in unsaturated soils coupled with a diffusive propagation in saturated soils.

The scheme proposed by Iverson has been adopted in D'odorico et al (2005) to investigate the effect of hyetograph characteristics on landslide potential.

For taking into account of hydrological phenomena Arnone et al. (2011) proposed the tRIBS model (Triangulated Irregular Network Real-Time Integrated Basin Simulator) that allows simulation of most of spatial-temporal hydrologic processes (infiltration, evapotranspiration, groundwater dynamics and soil moisture conditions) that can influence landsliding.

Most of the aforementioned approaches rely on the restrictive assumption of a steady-state subsurface flow, which can affect the predictive capability of the models both in terms of accuracy and timing of the prediction. Any model must always be validated regardless the implemented schemes by checking, for example, the accuracy of the simulation with the available experimental data or real case. The results can sometimes be very different applying different models to the same event, how described in Sorbino et al (2010) that illustrate how applying three different physically based models (SHALSTAB, TRIGRS and TRIGRS-unsaturated) on the same set of geo-environmental cases different results were obtained. The results reveal the advantages and limitations of each model in landslide forecasting.

For sure, these types of spatial distributed modeling are well-suited for shallow landslides but in larger landslides their efficiency is decreased by the higher complexity of the phenomena (van Westen et al.2003).

A detailed analysis of the individual mechanisms which occur in favor of landslide triggering is required for proper investigation by using complete models that can reproduce the spatial and temporal pattern of water flows in very well detailed domains.

In this work the complete model named SUSHI, **S**imulation for **S**aturated **U**nsaturated **H**illslope **I**nstability, (Capparelli and Versace, 2011) is applied in a very complex case to improve the understanding of the slope failure mechanism during rainfall infiltration.

SUSHI model takes into account several components, as specific site conditions, mechanical, hydraulic and physical soil properties, locale seepage conditions and their contribution to soil strength.

It is composed by a hydraulic module, to analyse the subsoil water circulation due to the rainfall infiltration under transient conditions and by a geotechnical module, which provides indications regarding the slope stability starting from limited equilibrium methods.

The hydraulic process is illustrated by the implementation of finite difference procedure that solves Richard's equation which is used to represent saturated/unsaturated flow within a hillslope. The temporal and spatial distribution of moisture content in subsurface are performed in order to evaluate different contribution as downslope and vertical components in flow regime in hillslope by unsteady rainfall.

Furthermore, the model was developed in order to be suitable for cases with strongly heterogeneous soils, irregular domains and boundary conditions variable in space and time. After a brief description of the model, the paper describes the analysis and the representative results obtained for the volcaniclastic covers of Sarno (Campania region - Southern Italy), where dangerous mud flows occurred in May 1998.

2 SUSHI model framework

The model is based on the combined use of two modules: HydroSUSHI, aimed at studying subsoil water circulation and GeoSUSHI, suited for evaluating the degree of slope stability. Infiltration analysis is carried out by using Richards' equation (1931), expressed as pressure-based methods to enable applications for layered soils and transient flow regime for both saturated and unsaturated conditions.

HydroSUSHI analyses subsoil water circulation in a spatial 2D domain which can be characterized by irregular soil stratigraphy with different hydrogeological properties.

By adopting a Cartesian orthogonal reference system Oxz, with z-axis positive downwards, the governing differential equation is:

$$\vec{\nabla}\left[K(\psi)\vec{\nabla}(\psi - z)\right] = \left[C(\psi) + S_e(\psi)S_s\right]\frac{\partial \psi}{\partial t} \quad (1)$$

where $K(\psi)[L/T]$ is the hydraulic conductivity which depends on pressure head $\psi[L]$ for unsaturated soils (ignoring soil anisotropy). The formula on the right was modified to simulate water flow in both unsaturated and saturated zones, so avoiding the use of different algorithms for the resolution of parabolic and elliptic equations respectively (Paniconi et al., 1991). $C(\psi) = \partial \vartheta / \partial \psi$ [L^{-1}] is specific soil water capacity in the unsaturated zone, which represents the rate at which a soil absorbs or releases water when there is a change in pressure head; $S_S\left[L^{-1}\right]$ is the specific volumetric storage. Effective Saturation $S_e[\psi] = (\vartheta - \vartheta_r)/(\vartheta_s - \vartheta_r)$, where θ is the water content, θ_s is the porosity and θ_r is the residual water content, can be computed using the Soil Water Retention Curve (van Genuchten and Nielsen, 1985). The saturated flow equation is simply a special case of Richards's equation in which the conductivity and storage terms are not functions of pressure head.

Recently, this module was upgraded through the integration of a method for the evapotranspiration process description, even if this component usually produces secondary effects when slope mobilizations occur in very rainy periods (Capparelli and Versace 2011). Since the study case proposed in the paper develops into a winter season, the effects related to evapotranspiration were neglected, because totally irrelevant in understanding the dynamics occurred.

Richards' equation does not allow analytical solutions unless in cases where simplifying hypotheses and /or particular boundary conditions are introduced, (Iverson, 2000; Srivastava e Yeh,1991). In HydroSUSHI module the finite differences (FDM) scheme and the fully implicit method are adopted.

Examples of finite difference algorithms which deal either variably saturated or fully unsaturated conditions are proposed by Freeze (1978) and Vauclin et al. (1979). The finite-difference method is one of the oldest numerical methods known for solving partial differential equations (pde). In this approach, the continuous problem domain is discretized so that the dependent variables are considered to exist only at discrete points.

Figure 1 draws an example of spatial discretization which is composed by regular mesh $\Delta x;\Delta z$. The size to be assigned to $\Delta x;\Delta z$ should be suitably selected depending on the complexity of the stratigraphy. It is important, in fact, to ensure a faithful reproduction of the layers, so as to guarantee a realistic representation of water flow exchanges.

With reference to the generic node with coordinates $x = x_0 + i\Delta x$, $z = z_0 + j\Delta z$ according to the finite difference scheme, the equation 1, can be written as:

$$\frac{1}{\Delta x}\left[K\left(\psi_{i+1/2,j}^{(k+1))}\right)\left(\frac{\psi_{i+1,j}^{(k+1)}-\psi_{i,j}^{(k+1)}}{\Delta x}\right)-K\left(\psi_{i-1/2,j}^{(k+1))}\right)\left(\frac{\psi_{i,j}^{(k+1)}-\psi_{i-1,j}^{(k+1)}}{\Delta x}\right)\right]$$
$$+\frac{1}{\Delta z}\left[K\left(\psi_{i,j+1/2}^{(k+1)}\right)\left(\frac{\psi_{i,j+1}^{(k+1)}-\psi_{i,j}^{(k+1)}}{\Delta z}-1\right)-K\left(\psi_{i,j-1/2}^{(k+1)}\right)\left(\frac{\psi_{i,j}^{(k+1)}-\psi_{i,j-1}^{(k+1)}}{\Delta x}-1\right)\right]$$
$$=C_{SU}\left(\psi_{i,j}^{(k+1)}\right)\left(\frac{\psi_{i,j}^{(k+1)}-\psi_{i,j}^{(k)}}{\Delta t}\right) \tag{2}$$

where $C_{SU} = \left[C(\psi) + S_e(\psi)S_s\right]$, the subscripts $i \pm 1/2, j$ and $i, j \pm 1/2$ indicate quantities evaluated at the spatial coordinates $\left(x_0 + (i \pm 1/2)\Delta x, z_0 + j\Delta z\right)$, and $\left(x_0 + i\Delta x, z_0 + (j \pm 1/2)\Delta z\right)$, Δt is the time step, the superscripts (k) and $(k+1)$ indicate quantities referring to time instants $t = t_0 + k\Delta t$ and $t = t_0 + (k+1)\Delta t$.

To solve the equation (1) boundary conditions along the edges of the domain problem must be specified. A general form of the boundary conditions for this pde can be written (McCord, 1991):

$$\alpha(\zeta)\psi + \beta(\zeta)\left.\frac{\partial\psi}{\partial n}\right|_{\partial G} = B(\zeta, t) \tag{3}$$

where $\alpha(\zeta), \beta(\zeta)$ and $B(\zeta, t)$ are given functions evaluated on the boundary region ∂G, the expression $\partial / \partial n$ is normal derivative operator and ζ it spatial local vector.

By applying this general formulation for water flow modelling the conditions become (figure 1): along the basal impermeable boundary BC and vertical boundary AB a Neumann condition in considered, whit flux equal to zero , then $\alpha(\zeta)=0, \beta(\zeta)=K(\zeta)$ and $B(\zeta,t)=q(\zeta,t)=0$. In terms of total hydraulic head $h=\psi+z$:

$$\left.\frac{\partial h}{\partial z}\right|_{BC}=0 \tag{3.1}$$

$$\left.\frac{\partial h}{\partial x}\right|_{AB}=0 \tag{3.2}$$

For vertical down-slope side DC we take into account the influence of the increasing subsurface flow, by considering both situations of unsaturated and saturated layers. This is computed by adopting boundary conditions moving from Neumann to Dirichlet condition, with specified flux or pressure head respectively, $\alpha(\zeta)=1, \beta(\zeta)=0$ and $B(\zeta,t)=h(\zeta,t)$. Then:

$$\left.\frac{\partial h}{\partial x}\right|_{DC}=q(x,t)=0 \tag{3.3}$$

$$\left.\psi\right|_{DC}=0 \tag{3.4}$$

On the upper boundary AD we allow a time-dependent rainfall $r[L/T]$. The boundary condition can be stated by considering the infiltration rate $I(x,t)$ as:

$$I(x,t)=K(x,t)\left.\frac{\partial h(x,t)}{\partial z}\right|_{AD} \tag{3.5}$$

In particular:

$$\begin{cases} I(x,t)=r(x,t) & if \quad r(x,t)\le K(x,t)\dfrac{\partial h(x,t)}{\partial z} \\ I(x,t)=K(x,t)\dfrac{\partial h(x,t)}{\partial z} & if \quad r(x,t)> K(x,t)\dfrac{\partial h(x,t)}{\partial z} \end{cases} \tag{3.5a}$$

The value $K(x,t)$ will depend on the values of $\psi(x,t)$ at the point x at time t and on the nature of the $K(\psi)$ curve for the surface soil at x.

Validation tests were carried out by the comparison of HydroSUSHI outputs with experimental solutions proposed in Vauclin et al. (1979), in Paniconi & Putti (1994) and with the suction data collected by the jet fill tensiometers located in a pilote site (Capparelli and Versace, 2011). The comparison of results for both applications was satisfactory and confirmed the capability of the model to simulate groundwater circulation.

Concerning GeoSUSHI module, stability analysis is performed for better understanding of the role of negative pore-water pressures (or matric suction) in increasing the shear strength of the soil.

It may be a reasonable assumption to ignore negative pore-water pressures for many situations where the major portion of the slip surface is below the groundwater table. However, for situations where the groundwater table is deep or where concern is over the possibility of shallow failure surface, negative pore-water pressures can no longer be ignored.

Recently Lu and Godt (2013) present an interesting work on understanding and quantifying the hydro-mechanical processes for predicting the spatial and temporal occurrence of landslide. The Authors provide quantitative treatments of rainfall infiltration, effective stress, their coupling and roles in hillslope stability, by introducing a unified effective stress framework linking soil suction to effective stress.

The procedure here proposed is an extension of conventional limit equilibrium methods adapted for the unsaturated soils as suggested by Fredlund and Rahardjo (1993).

The shear strength of an unsaturated soil can be formulated in terms of independent stress state variables $(\sigma - u_a)$ and $(u_a - u_w)$ as follows:

$$\tau_{ff} = c' + (\sigma_n - u_a)_f \tan\phi' + (u_a - u_w)_f \tan\phi^b \tag{4}$$

where the subscripts f indicate quantities evaluated at on the failure plane at failure, the τ_{ff} is shear stress, c' is effective cohesion, $(\sigma_n - u_a)_f$ net normal stress state, u_a pore-air pressure, ϕ' effective friction angle, $(u_a - u_w)$ matric suction, ϕ^b angle indicating rate of increase in shear strength relative to the matric suction. In practical applications, this last term is evaluated using the expression proposed by Vanapalli et al. (1996). The equation (4) is an extension of shear strength equation for a saturated soil. As the soil approaches saturation, the pore-water pressure, u_w, approaches the pore-air pressure u_a and matric suction $(u_a - u_w)$

goes to zero. The General Limit Equilibrium method (i.e GLE) provides a general theory wherein other methods can be viewed as special cases. It's well known, the elements used in GLE method for deriving the safety factor (FS) are the summation of forces in two directions and of the moments about a common point (Fredlund and Rahardjo;1993).Calculations for the stability of a slope are performed by dividing the soil mass above the slip surface into vertical slices. The mobilized shear force at the base of a slice can be written using the shear strength for an unsaturated soil:

$$S_m = \frac{\beta}{FS}\left[c' + (\sigma_n - u_a)\tan\phi' + (u_a - u_w)\tan\phi^b\right] \quad (5)$$

where S_m is the shear force mobilized on the base of the slice; β sloping distance across the base of a slice; FS safety factor which defined as the factor by which the shear strength parameters must be reduced in order to bring the soil mass into a state of limiting equilibrium along the assumed slip surface.

3 General description of the investigated context.

The case study proposed in the paper is located in Campania region (Southern Italy), where catastrophic flowslides and debris flows in pyroclastic soils are very usual. A brief list of some recent events is reported in Table 1 which includes also information about the size of the landslide.

Pizzo d'Alvano is a NW-SE oriented morphological structure, consisting of a sequence of limestone, dolomitic limestone and, subordinately, marly limestone dating from the Lower to Upper Cretaceous age. The slopes are mantled by very loose pyroclastic soils that are the result of explosive activity of the Somma-Vesuvius volcanic, both as primary air-fall deposits and volcanoclastic deposits, according to the mode of transport and deposition (Rolandi, 1997).

Air-fail deposits were dispersed from N-NE to S-SE, according to prevailing wind direction and covered a wide area reaching distances up to 50 km. Pumiceous and ashy deposits belonging to at least 5 different eruptions were recognized. From the oldest to the youngest, they are: Ottaviano (8000 years b.p.; E-NE dispersion direction), Avellino (3800 years b.p.; E-NE dispersion direction), 79 A.D. (E-SE dispersion direction), 472 A.D. (N-NE dispersion direction), 1631 A.D. (N-NE dispersion direction). The deposits are affected by pedogenetic processes determining paleosoil horizons during rest phases of the volcanic activity. The total thickness of the pyroclastic covers in these areas ranges between few decimetres to 10 meters, near to the uppermost flat areas. The general structure of the soil progressively adapts itself to the morphology of the calcareous substratum showing, therefore, complex and variable geometries (Rolandi,1997)

3.1 Shallow landslide events and main interpretations

On May 5, 1998, a huge number of mud flows were triggered on the slopes of the Pizzo d'Alvano massif, (Figure 2) involving an extension area of around 60 Km^2, a volume of 2.000.000 m^3 (40% derived from the eroded materials along the channels) and causing 165 victims and huge damages to urban centres Sarno, Quindici, Siano and Bracigliano.

These landslides were classified as very rapid to extremely rapid soil slip/debris flows (Ellen e Fleming, 1987) that travelled down-slope and then propagated in highly urbanized areas.

A characteristic element is the run-out distances that ranged from a few hundred meters up to distances greater than 2 km (Revellino et al.,2004) and speeds that, at the toe of channels, were estimated to be in the range of about 5–20 m/s.

Many similar phenomena have afflicted various other parts of the world, (Japan in 1985, the west coast of United States – California (1973, 1982, 2005), Brazil (1967), Venezuela (1999) sometimes involving similar pyroclastic soils. Even in Italy, as the disastrous mudslide with a volume of 180.000 m^3 which completely destroyed the Val di Stava village (it was July 19, 1985), due to the failure of two settling basins for industrial use, which caused the death of 268 people .

Although the triggering mechanism are different and sometimes the involved soils are not always similar, the common feature seems to be the presence of particles with a high porosity and a very low degree of cementation, which have a sudden change due to the action of an external agent (such as an earthquake or more often a rainfall event) which produces a rapid increase in pore water pressure.

A singularity of the landslides occurred in May 1998, which made the events even more tragic, is represented by their simultaneity; the distribution in time and space, the volume of material, take an unusual connotation. These phenomena are particularly dangerous and destructive due to the lack of clear warning signs, the high capacity erosive.

They were analyzed in several papers that indicate the most significant geomorphological, hydrological and geotechnical features of the involved slopes and models for the triggering mechanisms and propagation of landslides.

Cascini et al (2008) argue that the instabilities in Sarno was caused by a combined effect of water infiltrated in the surface layers and the one coming from the bedrock in correspondence to a temporary spring. This assumption was introduced considering, in the following years, springs from the bedrock were recorded during spring season. The main hypothesis is that the rainfall recorded in the hours immediately before the landslide events, has contributed to change the surface soil water circulation, in a slope already at limit of the equilibrium.

Calcaterra et al (2000) discuss the role played by grandwater circulation inside both the pyroclstic deposits and the karst cavities of the underlying limestone bedrock.

Even before the events of 1998, other Authors (Celico et al 1986) analyzing some events that occurred in pyroclastic covers in Campania region, have considered important not so much the previous daily rainfall as its relationship with the accumulated rainfall in the days or weeks before the landslide events.

The importance of soil water circulation is relevant due to the typical stratification pyroclastic covers, where one or more layers of pumice, with high permeability and layers of paleosoils, with lower permeability, are present. This situation encourages, when persistent rainfall events occur, runoff sub-surface conditions that may predispose to the slope instability in limited area. There is also discussion between who supports the importance of vegetation and plant roots and analyzes the possible relations with the instability (Mazzoleni et al, 1998). They emphasize the highly dynamic nature of the whole soil-vegetation, in which the hydrological processes can vary greatly as a result of the dynamics of vegetation. Abrupt changes in vegetation cover can produce equally rapid effects on soil and water regime.

Other authors, however, emphasize the role of the suction levels both to explain the trigger mechanisms and the condition that guarantees the stability in high slope (Greco et al., 2013).

Among the reasons, many authors have emphasized the importance of liquefaction with the sudden change of the soil, a structure initially characterized by a solid skeleton with a flow characterized by a fluid-like behavior (Olivares and Picarelli 2003).

3.2 In-situ conditions and information about rainfall triggering event

In the years following the landslide events, many filed surveys have been carried out in these areas, in order to assess the nature of the soil, the hydraulic and geotechnical characteristics.

For assessing the influence in the triggering mechanism, suction measurements were also performed along the Tuostolo basin (Sarno area), very close to areas collapsed in May 98 (Cascini e Sorbino, 2004), using “Quick-Draw” portable tensiometers and “Jetfill” in-place tensiometers.

These measurements were taken at three sites (Figure 3), at different depths from the ground surface. In particular, site n.1 was located in an area not affected by the landslides in 1998; sites 2 and 3 in landslide source areas. A significant data scattering can be noted (Figure 4), essentially related to the differences among the sites, the depths at which the measurements were carried out, and also to the local factors that induce changes at the end of the dry season when the acquired data show suction levels very high (around 65 kPa). The data also confirm a high sensitivity of the safety factor regarding the values of the cohesion instead of change in friction angle. The pyroclastic deposits covering the affected areas rest on slopes with high slope angles greater than 40 ° and also have thicknesses ranging from a few centimetres to few meters. In such geomorphological conditions, the soil suction, which increases the shear strength, is a major contributor to the stability, especially at slopes higher than the friction angle of the involved soils. The in-situ investigations show how the pyroclastic covers have friction angles between 32° and 38° and effective cohesion ranging from 0, pumice not reworked, to 4 -5 kPa for the ashy layers. These considerations justify the interest for the suction assessment in these pyroclastic soils as a major predisposing cause, if not the largest. The availability of models able to simulate the circulation of water in these complex terrains can provide useful tool for better understanding these phenomena.

The rainfall data was recorded by Sarno - Santa Maria La Foce rain gauge, located at 192m a.s.l , lower than the landslide source areas ,700m a.s.l.

The rainfall event, occurred on May 1998, has not been significant, revealing return period less than 5 years, but the period when it occurred makes it remarkable.

In fact, the monthly values of April and May in 1998 are significantly higher than the mean rainfall and the maximum daily rainfall values over 1967-1997 (Table 2). Also, on May 98, the rainfall has been recorded mostly in the first six days, with a total 114.6 mm. (Figure 5).

4 Sushi model application

Sushi model described was applied to the mudflow occurred in Tuostolo basin, highlighted by the red square in Figure 2, which destroyed Sarno village.

The actual geometry of the mudflow is the result of the coalescence of more landslides succeeded over a period of 6-8 hours.

The landslide has mobilized a volume of about 92,000 m3 of volcaniclastic materials resting over carbonate bedrock, including the eroded material within the channel. It developed, from an altitude of about 725 m, to the morphological frame, represented by sub-vertical limestone wall which is situated at an altitude of about 500 m (Figure 6).

Most of the landslide occurred on May '98, started just in correspondence of discontinuity morphological, also represented by topographic variations or anthropogenic discontinuity such as roads.

The application was developed with the aim of establishing an interpretative model of the triggering phase of the mudflow and its relations with the infiltration of rainwater in the pyroclastic covers.

4.1 Input data and slope scheme

To define the dynamics of the water circulation in the subsoil, the solution process requires the description of the investigated domain, the soil water characteristic curves, the permeability functions, the mechanical properties of the involved soils, the boundary and initial conditions.

Surveys and studies carried out by using also information available in the literature indicated the presence of alternating layers of pumice with a composition and thickness related to the characteristics of the eruptions and to the distance from the eruptive centres.

This sequence comprises both primary air-fall and volcanoclastic deposits. The primary deposits are composed by alternating layers of pumice, with interbedded paleosoils. At the basis of this sequence, above the bedrock, there is a layer of red-dark clayey ashy soil ("*regolite*") with rare limestone fragments.

By using the available topographic maps showing the ground top surface before the events, the stratigraphy was acquired.

At the main scarp, the average thickness of the pyroclastic cover is about 4 m. From top to bottom under a top soil formed by humified ashes including roots and organic matter (about 90 cm thick), the following layers were identified: (A) an upper layer (60 cm) of coarse pumices; (B) a layer (70 cm) of paleosoil; (C) a horizon (60 cm) of finer pumices; (D) a layer (80 cm) of paleosoil;(E) a bottom layer (40 cm) of weathered red-dark clayey ashy in contact with the fractured limestone bedrock (Figure 7).

In order to determine the mechanical and hydraulic properties of the involved cover, unisturbed specimens were collected, both in the investigated area and in other triggering areas belong to Pizzo d'Alvano slopes. Table 3 reports the mean values of physical properties of the different materials.

The hydraulic properties of the ashy soils in saturated conditions were investigated by means of conventional permeameter tests. In the unsaturated conditions, Suction Controlled Oedometer was utilized.

The experimental data were fitted by the expression proposed by van Genuchten and Nielsen (1985). (*Top soil*: $n = 1.6$ $m = 0.38$; *layer A*: $n = 1.71$ $m = 0.42$; *layer B*: $n = 1.66$ $m = 0.40$; *layer C*: $n = 1.8$ $m = 0.44$; *layer D*: $n = 1.9$ $m = 0.47$; *layer E*: $n = 2$ $m = 0.50$)

As can be seen in Figure 8, the obtained SWRC is typical of coarse soils with a low air-entry value, a low value of residual water content and a steep slope of the curve within the transition zone.

The values of the bubbling pressure, or air-entry tension, ψ_b, were determined through the graphic method proposed by Fredlund and Xing (1994). (*Top soil*: $\psi_b = 1.65(kPa)$; *layer A*: $\psi_b = 0.2(kPa)$; *layer B*: $\psi_b = 2.5(kPa)$; *layer C*: $\psi_b = 0.3(kPa)$; *layer D*: $\psi_b = 2.5(kPa)$; *layer E*: $\psi_b = 2.7(kPa)$)

The variable boundary conditions have been provided by using both Dirichlet and Neumann conditions. On the top (i.e. on the ground surface) flux boundary condition equal to rainfall infiltration capacity was performed; the runs allow to define step by step the infiltration rate for each node of the domain; on the bottom (i.e. at the contact between the pyroclastic cover and the bedrock) no flux was imposed, since the bedrock was assumed impervious; similarly for the upslope left side, a Neumann condition of no water flow was fixed, since the morphology of the analysed area makes reasonable the hypothesis of coincidence between the superficial and deep underground watershed so the contributions of fluxes coming from upstream may be assumed equal to zero; for the downslope right side, along the morphological frames, two different boundary conditions were imposed by using a Neumann or a Dirichlet condition if saturation occurs or not respectively.

For the slope section of Figure 7 the mesh was constituted by 130.000 nodes, according to the scheme known as mesh centered nodes, using regular quadrilateral with lengths and heights respectively equal to $\Delta x = 0{,}20m$ $\Delta z = 0{,}05m$

The initial conditions were defined in a non-arbitrary way, due to the data provided by the tensiometers that was located, as mentioned in section 3, very close to the selected study area. This information has been very useful for setting initial conditions. Constant distribution suction throughout the domain was firstly hypothesized by selecting, in particular, the following values:

$$\psi(x, z; t = 0) = 3;4;5;8;10;14 \quad [kPa] \tag{6}$$

By starting a simulation with no rain, a warm-up was performed for each of these values, to allow the redistribution of water content all over the domain. The equilibrium condition was reached when the standard deviation of the suction values in each node, is less than 10^{-5}.

The obtained distribution is compared with the available in-situ evidence recorded by tensiometers at the end of summer periods, because significantly comparable with the warm-up results. By comparing these profiles a strong similarity was evident with the distribution performed with $\psi(x, z; t = 0) = 6kPa$. This pore water pressure distribution was set as the initial condition for simulating the evolution between 1st October 1997 and 5th May 1998.

4.2 Groundwater modeling and slope analysis

The analyzed period was characterized by a total rainfall of 891 mm with greater values of rainfall intensity occurred between the end of October and December 1997.

Some diagrams were prepared to provide an example of results; they outline the conditions reached in two zones, considered as representative of the selected domain: one in the upslope part, at Z= 720*m* a.s.l. (hereafter referred to as "section A"), the other at the toe of the slope, at Z= 520*m* a.s.l, almost at the right boundary of the domain ("section B").

For each zone, the temporal distribution of suction profiles is drawn (Figure 9) plotting, in particular, the most critical profile computed for each month.

From Figure 9a it is evident that water table is not present at the top of the slope, since the values of the pressure head in the section are always lower than zero. This situation is fully congruent with the morphological characteristics of the zone, where steep slopes do not allow any form of accumulation. The situation is different for the Section B (Figure 9b), where the lower layers reach saturated conditions, and the upper ones present higher values close to saturation on 5th May. These results suggest that the saturation of the underlying layers was not the only cause of the instability of the slopes, even if it contributes to this phenomenon.

In fact, the suction levels seem to have played an important role for the mudflows occurred in May 1998. The values of rainfall heights during those days were not so extreme, but certainly unusual for a late spring period. The suction values achieved on May 1998 in the lower layers are not singular values: on the contrary, in previous periods the model provided quite similar distributions. The main difference lies in the fact that on 5th May 1998, the vertical profiles of water content present conditions close to saturation of the shallow layers.

This result is even more evident by analyzing the pressure profile along the slope and over the whole period considered. Figure 10 shows the pore-water pressures performed at 3 m and 0.7 m below the ground level. The first case represents a typical situation of a relatively deep layer, which reaches saturation in the first months of the rainy season and the second is representative of the conditions in the upper layers.

In the lower layers (Fig. 10a), the pressure levels remain approximately the same with the rainfall in late April and early May, while the upper layers (Fig.10b) get a sharp increase on May 5 . The values reached in the month of May in the lower layers are not singular values, in contrast, already at other times, the model refers distributions quite similar.

The substantial difference lies is that ever, as for May 5, in these distributions were added conditions close to saturation of the surface layers.

In relation to the computed pore pressure, slope stability analysis was carried out to simulate failure conditions and their correlation with increasing of soil water content.

Specifically, their effects on the stability were evaluated along several potential slip surfaces combining the results with infinite slope analysis methods, in order to present a predictive formulation of slope failures that occur as a result of rainfall events. In details, the analysis was evaluated in both saturated and unsaturated conditions by using an extension of Mohr-Coulomb criterion; at different depths from the ground surface the average value of pore pressure was calculated, and the correspondent value of FS was estimated using the method of infinite slope.

In details, for several depth from the ground level (0.3m, 0.7m, 1.8m, 2.1 m, 2.9m, 3.1m, 3.8m) the average value of pore pressure was calculated, and then the correspondent value of FS was estimated using the method of infinite slope. This method is the simplest limit equilibrium method for slope stability analysis and gives reliable results for slides where the longitudinal dimension prevails on the depth of the landslide, as for the landslide here analyzed.

The plots in Figure 11 provide the time sequence of the simulated FS values; these results can help in understanding the evolution of the slope stability conditions.

The values in the lower layers are always indicative of stability; lower values, but nevertheless above 1, are due to the greater thicknesses of coverage and higher values of pore pressure. In the more superficial layers the trends are more variable and reveal a depth of 0.7m, a decrease of FS value of 0.98 on May 5, 1998.

This result seems to be interesting, because suggest the hypothesis that the saturation of these deep layers is not the only reason of the slopes instability in the investigated context but, certainly, contributes to this phenomenon. The rainfall occurred on May 98, though not exceptional, are unusual for late spring; they significantly increased the level of pore water pressure in the upper layers, leading to a condition of instability.

5 Conclusions

The proposed SUSHI model is able to represent, with sufficient details, the phenomena induced by rainfall, in soils characterized by complex stratigraphy and hydraulic properties, and represents a complete model for water circulation analysis.

The application in the selected slope of Sarno area (Southern Italy) has enabled the reconstruction of the full development of pore pressures in colluvial layers and to distinguish the conditions occurred on May 1998 from the previous ones, thus providing important information to identify the possible critical conditions of these slopes. In particular, by analyzing the obtained results, the role of the suction appears to have been decisive for the triggering of landslide movements, consistently with the most reliable theories that attribute to the dynamics of water circulation in the surface soils a primer role either for the triggering phase and the subsequent propagation phase.

Further applications to cases recorded on 5th May 1998 and periods without landslides could certainly better delineate the critical conditions and provide useful information for a possible early warning system. As well further analyses should be carried out in order to better evaluate the influence of the bedrock, of the road cuts located in the upper zone of the triggering areas, and other factors that could have influenced the evolution of events.

References

Arnone, E., Noto, L.V., Lepore, C., and Bras, R.L.: Physically-based and distributed approach to analyze rainfall-triggered landslides at watershed scale, Geomorphology, n/a. doi: 10.1016/j.geomorph.2011.03.019, 2011

Baum, R.L., Savage, W.Z., and Godt, J.W.: TRIGRS - a FORTRAN program for transient rainfall infiltration and grid-based regional slope stability analysis, US Geological Survey Open-File Report, 02-0424, 2002

Baum, R.L., Godt, J.W., and Savane, W.Z.: Estimating the timing and location of shallow rainfall-induced landslides using a model for transient, unsaturated infiltration, J. Geophys. Res.,115:1-26, 2010.

Caine N.: The rainfall intensity-duration control of shallow landslides and debris flows, Geogr. Ann. 62A(1-2):23-27, 1980.

Iverson, R.M.: Landslide triggering by rain infiltration, Water Resour Res, 36: 1897-1910, 2000.

Capparelli G. and Tiranti D. Application of the MoniFLaIR early warning system for rainfall-induced landslides in the Piedmont region (Italy). Landslides 7 n.4, 401-410; Springer-Verlag. (2010) DOI: 10.1007/s10346-009-0189-9

Capparelli, G., and Versace, P.: FLaIR and SUSHI: Two mathematical models for Early Warning Systems for rainfall induced landslides, Landslides, 8: 67-79, 2011.

Cascini L, Cuomo S, Guida D:Typical source areas of May 1998 flow-like mass movements in the Campania region, Southern Italy. Eng Geol 96:107–125, 2008.

Calcaterra D., Parise M., Palma B. e Pelella L.: Multiple debris flows in volcanoclastic materials mantling carbonate slopes. Atti 2nd Int. Conf. “Debris-FIow Hazard Mitigation”, Taipei, Taiwan, 16-18 Luglio 2000, pp. 99-107. 2000. Balkema, Rotterdam.

Celico, P., Guadagno, F. M., Vallario, A.: Proposta di un modello interpretativo per lo studio delle frane nei terreni piroclastici, Geologia Applicata e Idrogeologia, 22, Bari, 1986

Dhakal, A.S. and Sidle, R.C. Pore water pressure assessment in a forest watershed: Simulations and distributed field measurements related to forest practices. *Water Resources Research 40.* (2004). doi: 10.1029/2003WR002017

D'Odorico, P., Fagherazzi, S. and Rigon, R. Potential for landsliding: Dependence on hyetograph characteristics. Journal of Geophysical Research 110. (2005). doi: 10.1029/2004JF000127.

Ellen S.D., Fleming R.W. (1987): *Mobilization of debris flow from soil slips, San Francisco Bay region, California*, Engineering Geology, 7 , 31-40.

Fredlund, D.G., and Rahardjo, H.: Soil Mechanics for Unsaturated Soils, John Wiley & Sons, 1993.

Fredlund, D.G., and Xing, A.: Equations for the soil-water characteristic curve, Can Geotech J, 31:521-532, 1994.

Freeze. RA. 'Mathematical models of hillslope hydrology", in Kirkby, MJ (Ed.), Hillslope Hydrology, John Wiley & Son 177-226., 1978.

Glade T. (2000): Modelling landslide-triggering rainfalls in different regions in New Zealand - the soil water status model.- Zeitschrift für Geomorphologie 122, 63-84.

Greco R., Comegna, L., Damiano E., Olivares, L., Picarelli L,:Hydrological modelling of a slope covered with shallow pyroclastic deposits from field monitoring data. Hydrol. Earth Syst. Sci. Discuss., 10, 5799–5830, 2013 doi:10.5194/hessd-10-5799-2013

Guzzetti, F.: Book Review of “Measuring Vulnerability to Natural Hazards”, Nat. Hazards Earth Syst. Sci. 8, 521, 2008.

Iverson, R.M.: Landslide triggering by rain infiltration, Water Resour Res, 36: 1897-1910, 2000.

Lu N. and Godt J. “Hillslope Hydrology and Stability” , Cambridge University Press, 2013

Martelloni G, Segoni S, Fanti R *et al*., 2011. Rainfall thresholds for the forecasting of landslide occurrence at regional scale. *Landslides*, doi: 10.1007/s10346-011-0308-2.

Mazzoleni, S., Strumia, S., Di Pasquale, G., Migliozzi, A., Amato, M., Di Martino, P.: Il ruolo della vegetazione nelle frane di Quindici. Tratto da: “L’instabilita` delle coltri piroclastiche delle dorsali carbonatiche in Campania: primi risultati di uno studio interdisciplinare”. 20 Rapporto informativo dellUnita`Operativa 4/21N del CNR/GNDCI, 1998.

Montgomery, D.R. and Dietrich, W.E: A physically based model topographic control on shallow landsliding, Water Resour Res, 30: 1153-1171, 1994.

Olivares, L. and Picarelli, L.: Shallow flowslides triggered by intense rainfalls on natural slopes covered by loose unsaturated pyroclastic soils, Géotecnique, 53(2): 283-288, 2003.

Pack, R.T., Tarboton, D.G. and Goodwin, C.N.: SINMAP, a stability index approach to terrain stability hazard mapping, SINMAP user’s manual, 68, Terratech Consulting Ltd, 1998.

Paniconi, C., Putti, M.,. A comparison of Picard and Newton iteration in the numerical solution of multidimensional variably saturated flow problems. *Water Resources Researches*, 30, No 12, 3357-3374,1994

Rahardjo, H., Li, X.W., Toll, D.G., Leong, E.C., 2001, The effect of antecedent rainfall on slope

stability. Geotechnical and Geological Engineering 19, 371–399

Revellino P, Hungr O, Guadagno FM, Evans SG: Velocity and runout simulation of destructive debris flows and debris avalanches in pyroclastic deposits, Campania region, Italy.

Environ Geol 45:295–311,2004.

Rigon, R. Bertoldi, G. and Over, T.M. 2006: GEOtop: A Distributed Hydrological Model with Coupled Water and Energy Budgets. *J. Hydrometeor*, **7**, 371–388.

Rolandi G. The eruptive history of Somma-Vesuvius volcanism and archeology in Mediterranean area. De Vito and Cortini (eds) 1997

Sorbino G., Sica C., Cascini L. Susceptibility analysis of shallow landslides source areas using

physically based models. Natural hazards, 53(2), 313-332 (2010).

Srivastava R., Jim Yeh T.C.,. Analytical Solution for One-Dimensional, Transient Infiltration Towards the Water Table in Homogeneous and Layered Soils. Water Resources Research, 27(5): 753-762, 1991

Tsai, T. L, Chen, H.E. and Yang, J.C.: Numerical modeling of rainstorm induced shallow landslides in saturated and unsaturated soils, Environmental Geology 55:1269-1277, 2008.

Vanapalli, S.K., Fredlund, D.G., Pufahl, D.E., and Clifton, A.W.: Model for the prediction of shear strength with respect to soil suction, Can. Geotech. J., 33, 379-392, 1996.

Van Genuchten, M.T., and Nielsen, D.R.: On describing and predicting the hydraulic properties of unsaturated soils, Ann Geophys 3(5): 615-628, 1985.

Van Westen, C. J., Rengers, N., and Soeters, R.: Use of geomorphological information in indirect landslide susceptibility assessment, Natural Hazards, 30, 399–419, 2003.

Vauclin, M., Khanji, D. e Vachaud, G.,. Experimental and numerical study of a transient, two-dimensional unsaturated-saturated water table recharge problem. *Water Resources Researches*, 15, No 5, 1089-1101, 1979

Wu, W., and Sidle, R.C.: A distributed slope stability model for steep forested basin, Water Resource Res 31: 2097-2110, 1995.

Table 1. Features of some recent flowslides in Campania Region (Versace et al., 2009)

Site	Date	Length (m)	Volume (m^3)
Ischia	2006	450	$3*10^4$
Cervinara	1999	$2*10^3$	$4*10^4$
Avella	1998	$15*10^2$	$2*10^4$
S. Felice a C.	1998	$8*10^2$	$3*10^4$
Sarno	1998	$2\text{-}4*10^3$	$5*10^5$
Bracigliano	1998	$1\text{-}2*10^3$	$15*10^4$
Siano	1998	$14*10^2$	$4*10^4$
Quindici	1998	$1\text{-}4*10^3$	$5*10^5$
Maiori	1954	10^3	$5*10^4$
Avellino	2005	$4*10^2$	$2*10^4$
Montoro Inf.	1997	$2*10^3$	$3*10^4$

Table 2. Comparison between monthly mean and daily maximum rainfall, computed for the period 1964-1997 and the year 1998

	Jan.	**Feb.**	**Mar.**	**Apr.**	**May**	**June**	**July**	**Aug.**	**Sept.**	**Oct.**	**Nov.**	**Dec.**
Monthly expected value (mm) 1964/1997	87	85	73	73	38	26	18	27	60	104	129	111
1998	77	46	44	**109**	**150**	12	6	39	122	52	124	94
Daily maximum (mm)	29	24	23	22	15	13	9	16	27	32	38	34
1998	42	21	13	**37**	**74**	6	5	20	47	17	25	37

Table 3. Average values of pyroclastic soil properties

Soil properties	*Top Soil*	*Pumice (A)*	*Paleosoil (B)*	*Pumice (C)*	*Paleosoil (D)*	*Regolite (E)*
Dry unit weight [kN/m^3]	*10.99*	6	7	6	9	10.75
Saturated unit weight [kN/m^3]	*17.2*	13	13	13	15	15.3
Saturated soil water content θ_s	0.55	0.82	0.61	0.68	0.61	0.60
Residual soil water content θ_r	0.14	0.23	0.18	0.05	0.18	0.10
Saturated hydraulic conductivity K_s [m/sec]	3.2E-05	1.0E-03	1.0E-06	1.0E-02	4.0E-06	7.6E-07
Effective coesion c'[kPa]	2	0	4.5	0	4.7	15
Friction angle ϕ' [°]	15	30	24	32	28	21

Figure 1. Nodal network implemented for development of FDM equation.

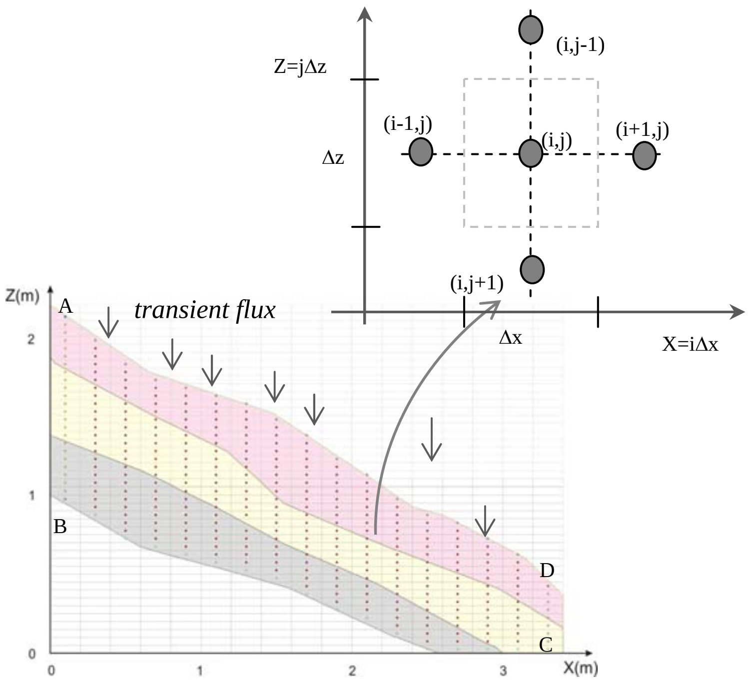

Figure 2. Overview of Pizzo d'Alvano massif and the area affected by the May 1998 mud flows. Red square delimits the analyzed event by Sushi model

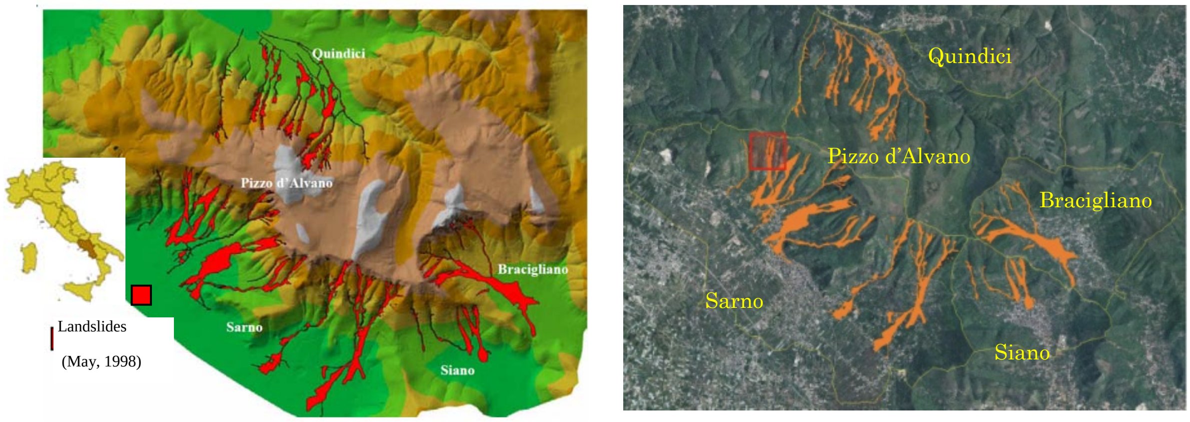

Figure 3. Topography map and sites where suction measurements were performed.

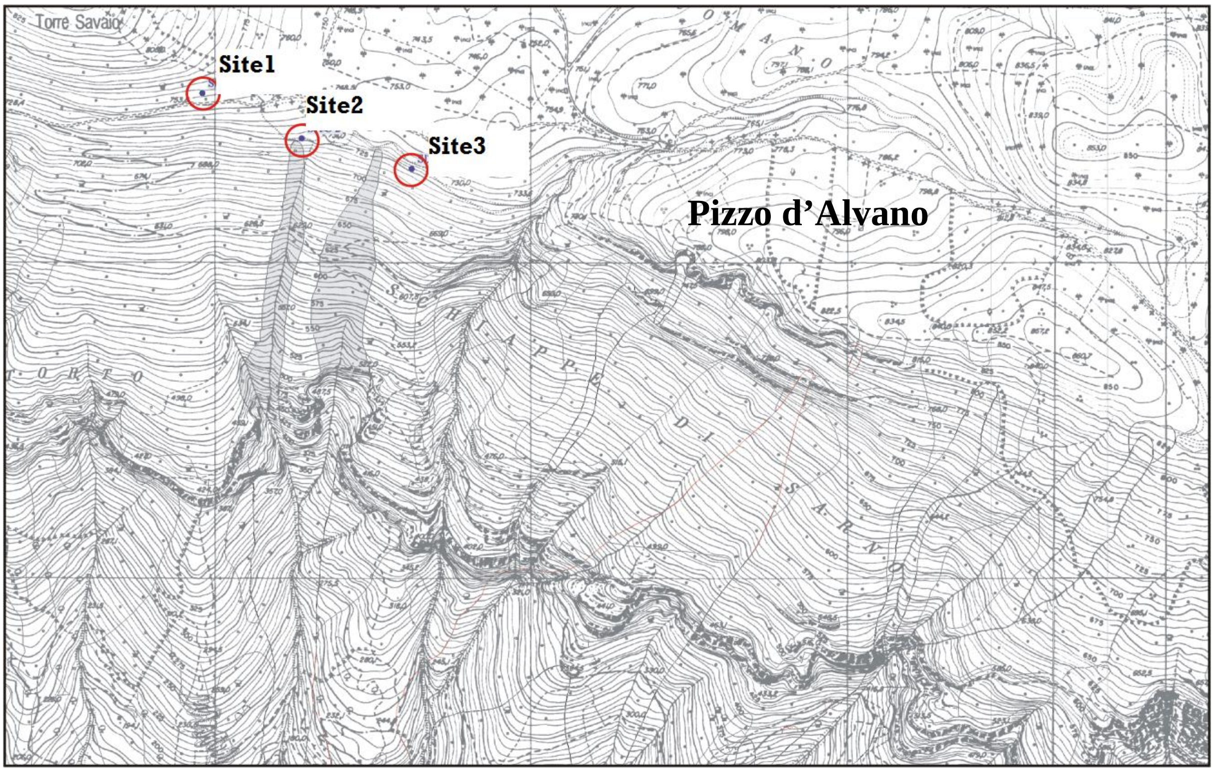

Figure 4. Suction trends recorded along sites at 0.20 m (a), 1.00 m (b), 1.60m (c) under the ground surface and daily rainfall by Santa Maria la Foce rain-gauge.

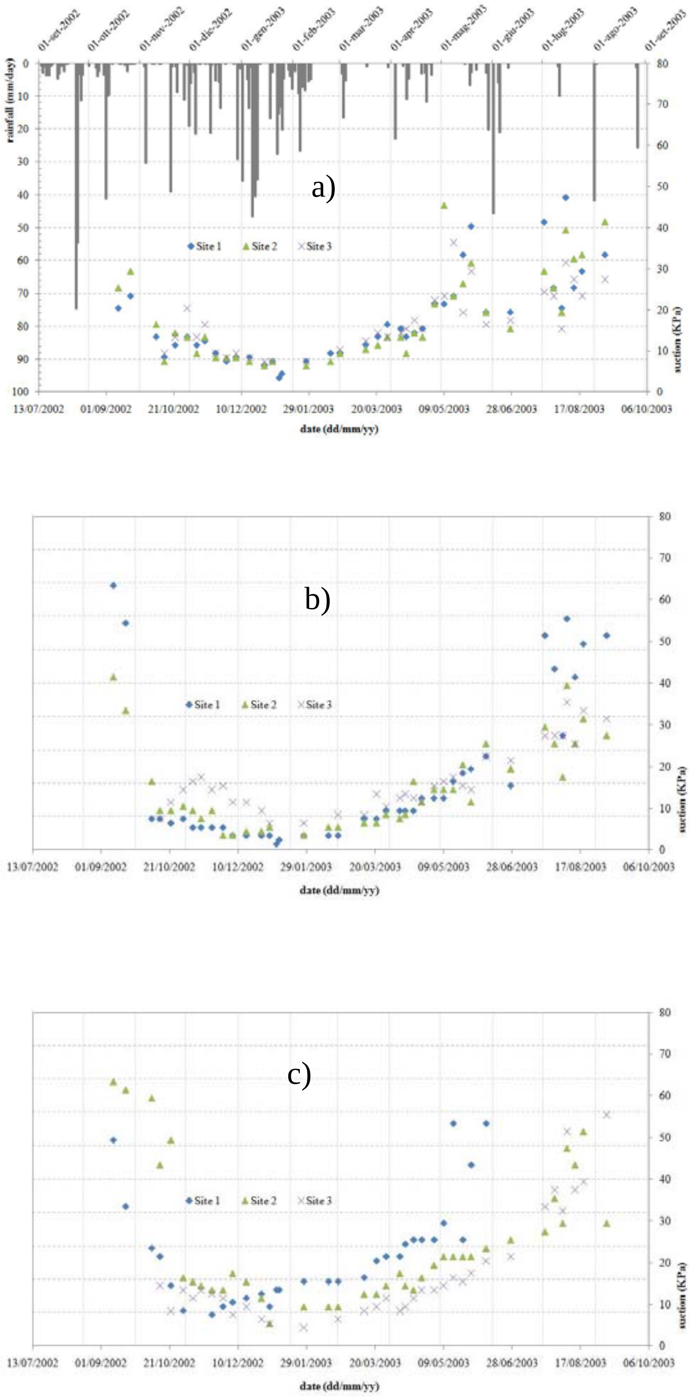

Figure 5. Comparison of daily and cumulative rainfall data recorded at Sarno- rain gauge in 1998.

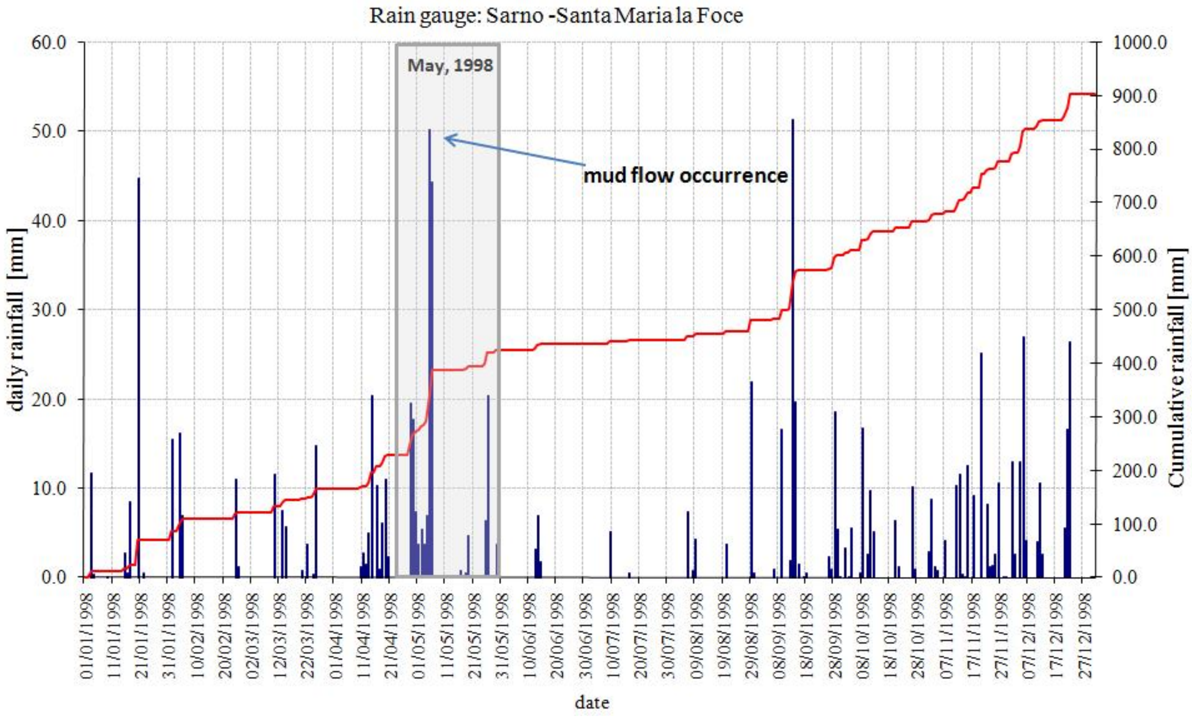

Figure 6. Detail pictures of case study.

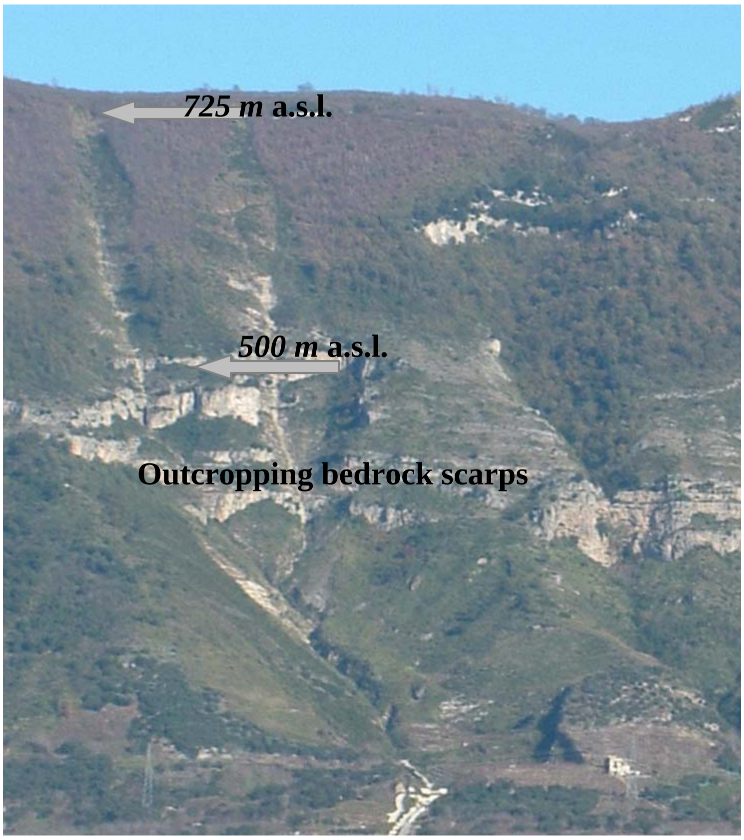

Figure 7. Geometric and stratigraphic characterization of the investigated slope

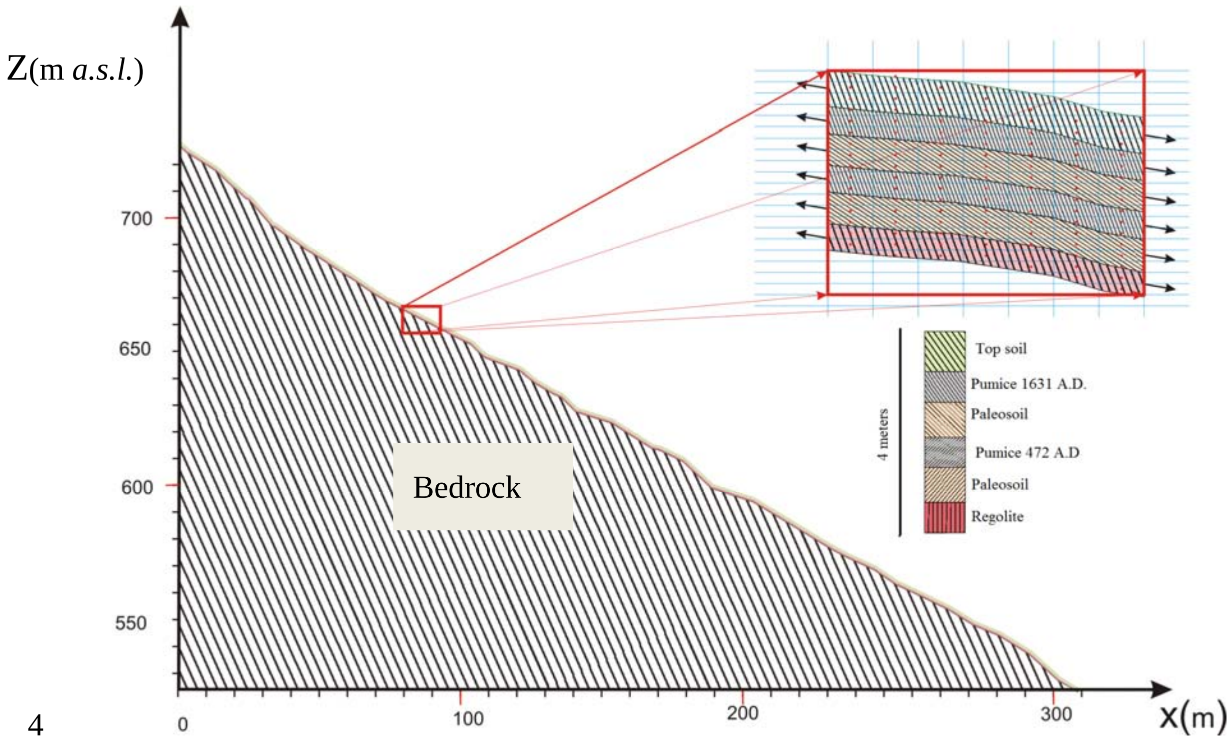

Figure 8 Soil water characteristic curves

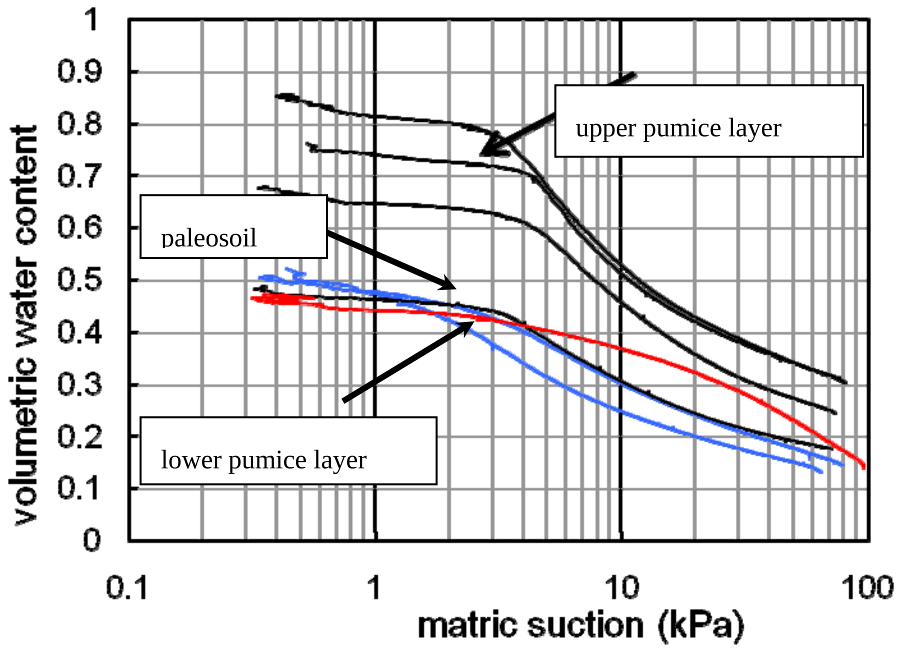

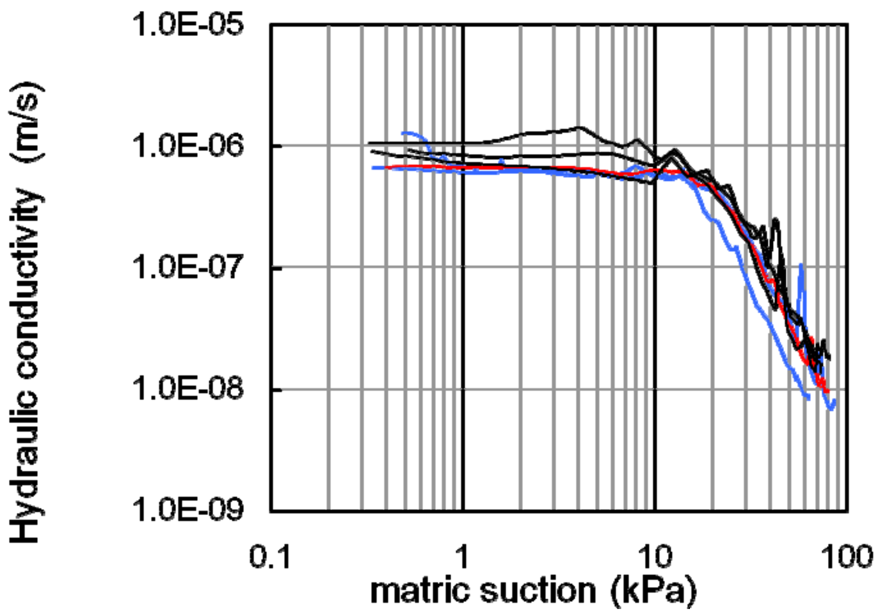

Figure 9. Computed suction profile for (a) the upslope section (Sect A) and (b)the downslope section (Sect B).

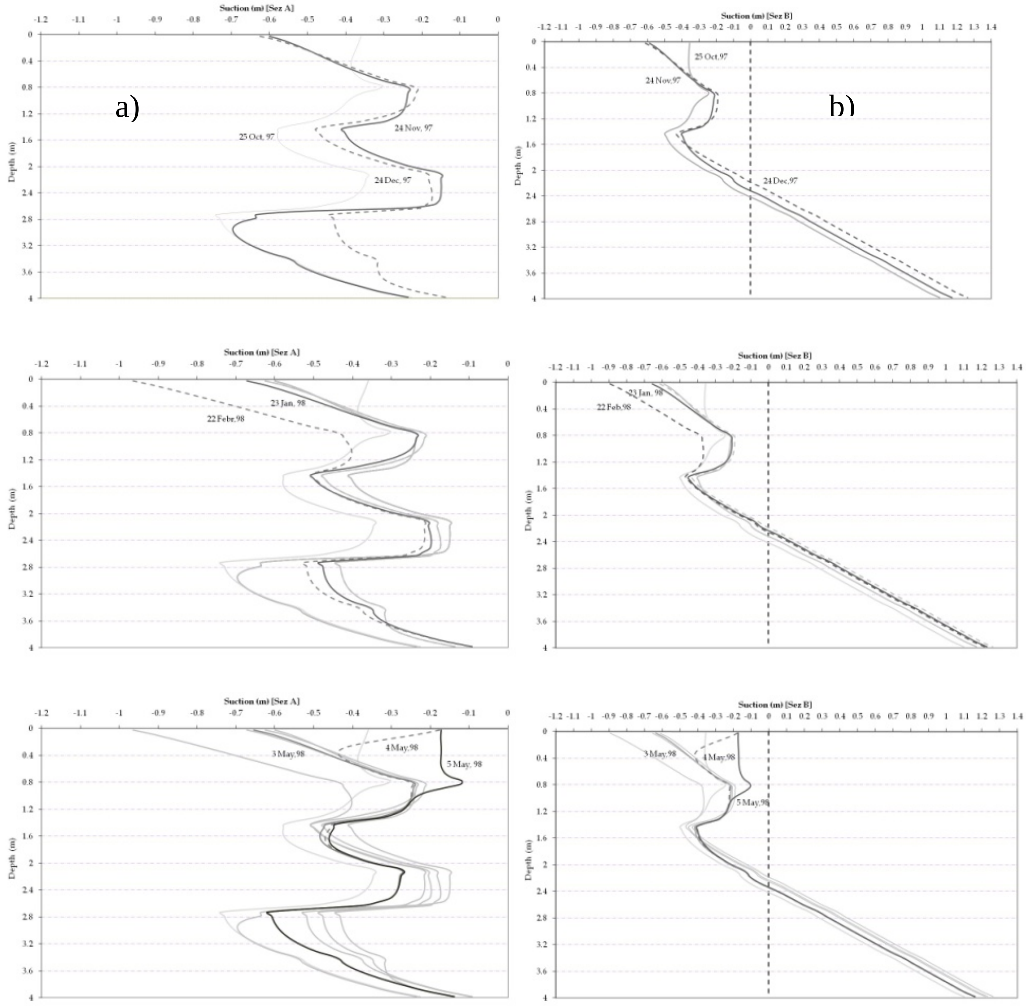

Figure 10 Pore-water pressures performed at (a) 3 m and (b) 0.7 m below the ground surface.

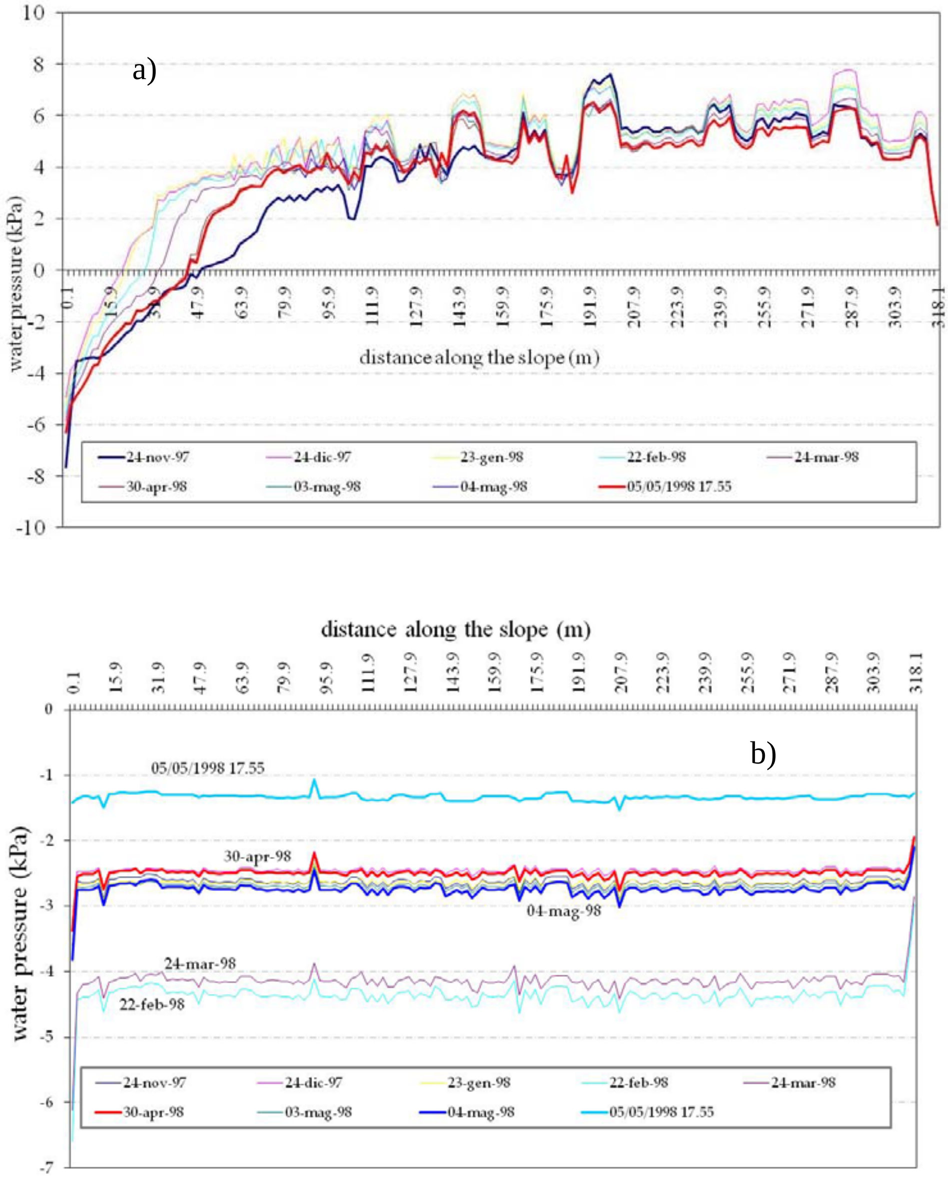

Figure 11 Slope safety factor depending on pore-water pressures performed and soil mechanism properties at different depths from the ground surface.